Journal of Geology & Geophysics
ISSN: 2381-8719

Benammi et al., J Geol Geophys 2017, 6:2
DOI: 10.4172/2381-8719.1000282

Research Article Open Access

Preliminary Magnetostratigraphic and Isotopic Dating of the Ngwa Formation (Dschang Western Cameroon)

Benammi M[1]*, Hell JV[2], Bessong M[2], Nolla D[2], Solé J[3] and Brunet M[1,4]

[1]*Institut de Paléoprimatologie, Paléontologie Humaine: Évolution et Paléoenvironnements (IPHEP), UMR-CNRS 7262, Bâtiment B35, 6 rue Michel.Brunet, 86022 Poitiers Cedex, France*
[2]*Institut de Recherches Géologiques et Minières du Cameroun, BP 4140, Yaoundé, Cameroun*
[3]*Universidad Nacional Autónoma de México, Instituto de Geología Dept. de Geoquímica Cd. Universitaria, Coyoacán 04510 México DF*
[4]*Collège de France, Chaire de Paléontologie humaine, 11 Place Marecelin Berthelot, 75231 Paris cedex 05*

Abstract

A magnetostratigraphic study has been carried out to constrain the age of the volcano-sedimentary Ngwa formation in the eastern part of the Dschang region. A stratigraphic section of about 80 meters thick corresponding to 26 sites has been sampled, and it is composed mainly of fine-grained sandstones, clays, lignite, volcanic sediment and tuffs. A magnetic study conducted on 56 samples shows one or two components of magnetization carried either by titanomagnetite, magnetite and Fe-sulphide. The section that was sampled shows one normal polarity and one reversed polarity. In the lower part of the section, a K-Ar radiometric dating was performed on the plagioclase minerals isolated from the tuffs level situated about 15 meters above the lignite seam, and gave an age of 20.1 ± 0.7 Ma. Constrained by this age, the observed polarity zones can be readily correlated with chrons C6An.1n-C6An.1r of the GPTS. This study suggests that the age of the lignite is comprised between 20.04 Ma and 20.21 Ma. The mean direction of the characteristic remanent magnetization documents a counterclockwise vertical axis rotation of about 8° with respect to the expected Lower Miocene direction derived from the Africa polar wander curve.

Keywords: Cameroon; Ngwa formation; Magnetostratigraphy; Lignite; Lower Miocene

Introduction

Most studied and well known continental basins from Cameroon are Mesozoic intracontinental basins such as Mamfe [1,2], Mbere Djerem [3,4], Babouri Figuil [5], Mayo Oulo Lere [6-8], Hamakoussou [9,10] and Mayo Oulo-Léré [6].

However, little attention has been paid to the continental Cenozoic sediments. Some fragmentary sediment lithofacies were identified at Ngwa Village (eastern Dschang) as well as some enclaves of sedimentary rocks randomly distributed in a volcanic complex [11]. However, very little is known about the features of these sedimentary rocks, their age or provenance. Research work started in 1925 in the Dschang area to assess the extent of the lignite deposits [12]. After several hundred meters of gallery and the test use of the lignite as a fuel, the exploitation was stopped because of the bad quality of the lignite. Capponi [12] suggested a Tertiary age for the Dschang lignite in comparison with lignite known in southern part of Nigeria. The lignite deposit is known also North-east of Bamenda, the strata there are vertical and overlaid by clays which are the product of basalt alteration. The lignite seams found in Dschang and Bamenda are commonly brownish to black in color and vary in thickness from a few centimeters to a maximum of 1.8 m. They are thinly laminated and contain fossils of leaves, fruits and wood fragments. Magnetic polarity sequences with K-Ar dating result will the calibration of the Ngwa Formation to the geomagnetic polarity time scale (GPTS). In this paper, we present magnetostratigraphic results of the Early Miocene section of the Ngwa Formation and its correlation to the GPTS. This study is of great importance, since it is the first one carried out in a Neogene continental formation of Cameroon.

Introduction to geological setting

The study was carried out in the area of Ngwa, a small locality in the eastern part of the Dschang region on the southern slope of Mount Bambouto belonging to the Cameroon Volcanic Line (CVL) (Figure 1). The CVL represents a 1600 km long chain of Cenozoic volcanic and sub-volcanic complexes that straddles the continent ocean boundary and extends from the Gulf of Guinea to the interior of the African continent [13]. It constitutes a major tectonic feature in Central Africa characterized by a zone of fault-bounded horsts and grabens that extend N30°E. These structures are thought to be induced by a network of combined faults, related to an intra-plate sliding system of high extension [14]. Its continental part is represented by the major volcanic massifs of Mounts Cameroon, Rumpi, Manengouba, Bambouto and Oku and the volcanic necks and plugs of the Kapsiki plateau and Benue Valley [15]. Mount Bambouto is the third largest volcano of the CVL after Mounts Cameroon and Manengouba [16]. According to Kagou Dongmo et al. [17], the geological history of Mount Bambouto is divided into three stages: 1) The pre-caldera stage corresponds to the building of the main shield volcano, between 21 and 16 Ma. It was mainly effusive and basaltic; 2) Collapse of a large caldera initiated the second stage characterized by the extrusion of ignimbritic trachytes, between 16 and 11 Ma [18]; 3) The post-caldera and third stage consists of the pouring out of intra-caldera and adventive basaltic flows, and of extrusions of phonolitic domes, between 9 and 4.5 Ma [13] (Table 1).

The Dschang region, on the southern slope of Mount Bambouto in the West Cameroon Highlands, forms the northern edge of the

***Corresponding author:** Benammi M, Institut de Paléoprimatologie, Paléontologie Humaine: Évolution et Paléoenvironnements (IPHEP), UMR-CNRS 7262, Bâtiment B35, 6 rue Michel.Brunet, 86022 Poitiers Cedex, France, Tel: + 56187897; Fax: +555502486; E-mail: mbenammi@univ-poitiers.fr

Received December 22, 2016; **Accepted** February 17, 2017; **Published** February 23, 2017

Citation: Benammi M, Hell JV, Bessong M, Nolla D, Solé J, et al. (2017) Preliminary Magnetostratigraphic and Isotopic Dating of the Ngwa Formation (Dschang Western Cameroon). J Geol Geophys 6: 282. doi: 10.4172/2381-8719.1000282

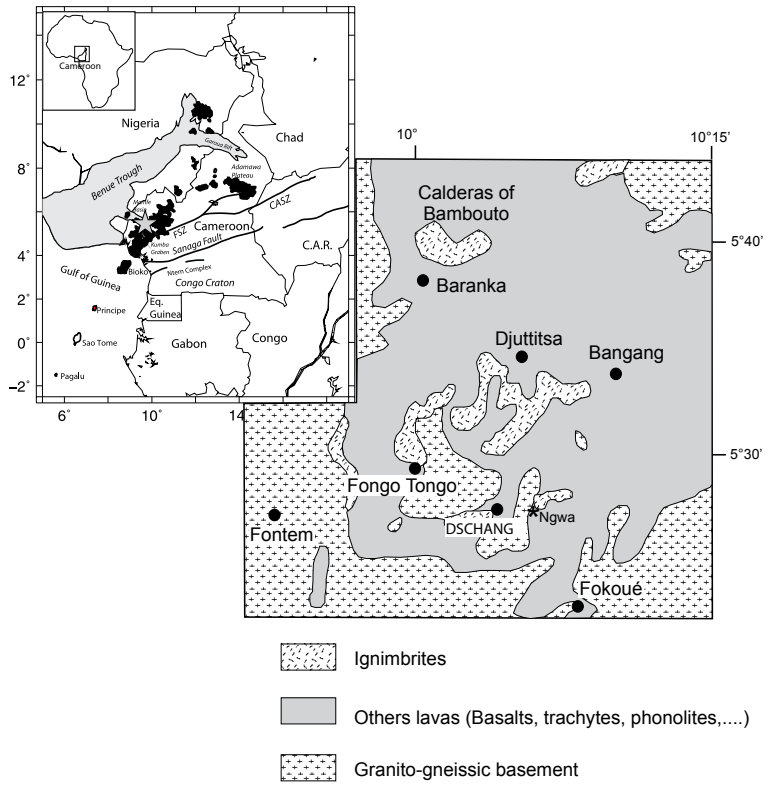

Figure 1: Sketch map of the central portion of the Cameroon Volcanic Line in West Equatorial Africa (see inset), FSZ, Foumban shear zone; CASZ, Central African shear zone. Geological sketch map of the Bambouto Mountains indicating the location of the study area [15].

Sample	Mineral	%K	$^{40}Ar^*$ (moles/g)	$\%^{40}Ar^*$	Age (Ma)
Cameroon	Plagioclase	0.984	3.45×10^{-11}	68.3	20.1 ± 0.7

Table 1: K-Ar datting of the volcanic tuff of Ngwa formation.

Mbo plain (Figure 1). It is characterized by various volcanic products covering the basement granitoids [11]. The basement rocks in the Dschang region consist of Neoproterozoic granite-gneisses, Late Proterozoic granitoids intruded within the granite gneisses and gabbroic dykes that crop out in the two previous units. The basement rocks are partly covered by a very thick layer of volcanic deposits derived from Mount Bambouto. Volcanic activity at Mount Bambouto originated as a complex sequence of basalt, trachyte and phonolite lava flows and ignimbrites [13,15,18,19].

The most important sedimentary rock outcrop is at the Ngwa locality in the eastern part of the Dschang region (Figure 1), and a number of small lignite deposits are encountered. The Ngwa Formation consists of a sequence of coarse-grained sandstone, brown and dark coloured clays and carbonaceous shale intercalated within lignite seams of continental origin. A sedimentological study was conducted by Kenfack et al. [11] who highlighted four lithofacies, and the volcanic sediment was related to volcanic activity at Mount Bambouto during the Miocene. This led to the deposition of volcano-clastic sediment which occurs at the base of the sedimentary sequence that unconformably overlys the Precambrian basement (Figure 5).

Description of the Ngwa section

The sedimentary succession exposed in the Ngwa corresponds to 80 m of lacustrine and volcano-clastic sediments belonging to the Ngwa Formation. The lower portion of the sequence is represented by an interstratified succession of conglomerate, clay, sand, volcanic sediment and lignite, all of variable thickness and texture. The conglomerate beds in the lower part lay on the granite substratum, and are composed of chert, quartz, lithic, and laterite clasts (Figure 5 and Figure 6A). The clasts don't exceed 5 cm in diameter. The conglomerate beds occur at distinct layers, but it is commonly present at the bases of sandstone units. Lignite is developed as stratified lignitic clays and marls or as massive lignite (Figure 5 and Figure 6B). They commonly contain well preserved macrofloral remains as the lignitic clays (leaves, fruits and wood). The absence of rooting structures indicates an allochthonous origin of macrofloral material. The sandstones are massive, and the bases of the beds are non-erosive. A fine grained yellowish tuff layer (about 2 m thickness) occurs above the basal conglomerate. This layer is called "Bamilékite" according to Capponi [12], and it marks a break slope in the section (Figure 6A). The overlying bed (nearly 40 m thickness) of the section is dominated by volcano-clastic sediment (Figure 5). All the section is covered by laterized soil. The soil cover is composed of massive unconsolidated and porous reddish brown laterized sandy clay.

Materials and Methods

Paleomagnetic sampling and sample analysis

A total of 29 cores (Figure 5) were drilled in the field from 19 levels with a portable gasoline powered drill and oriented in situ with

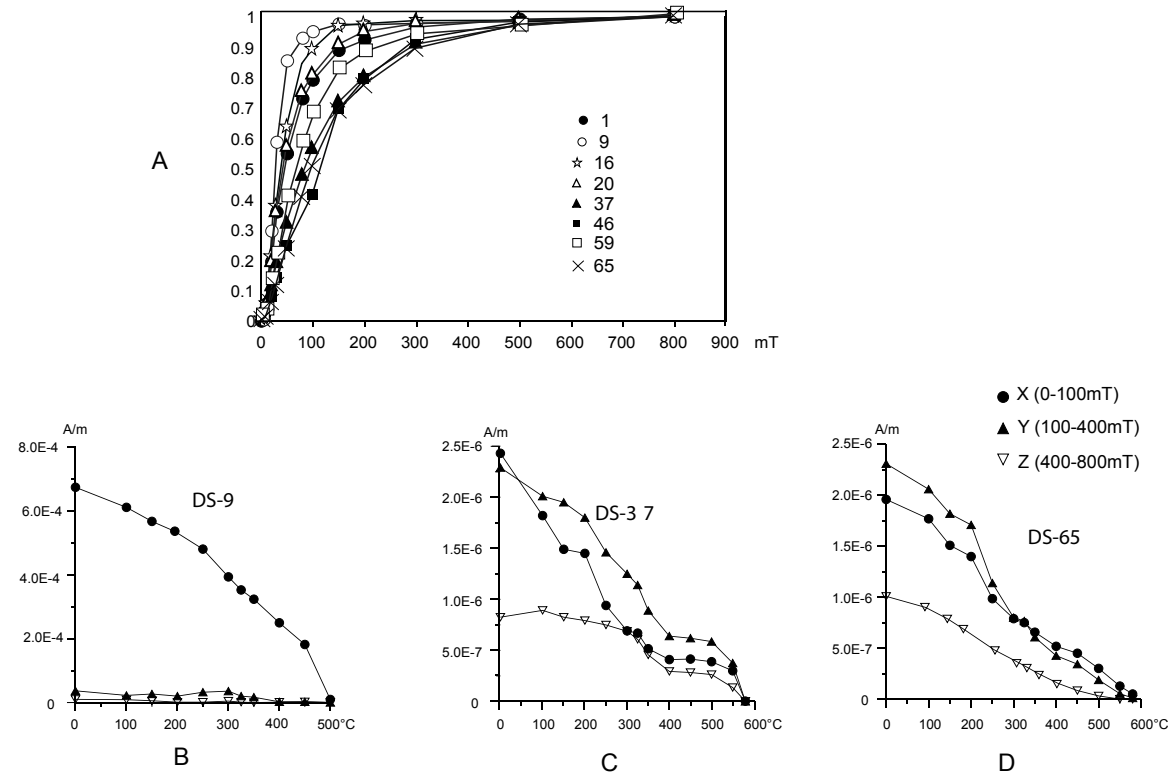

Figure 2: A) Progressive acquisition of an isothermal remanent magnetization in field of 800 mT. B-D): Thermal demagnetization of a composite IRM acquired on three orthogonal axes.

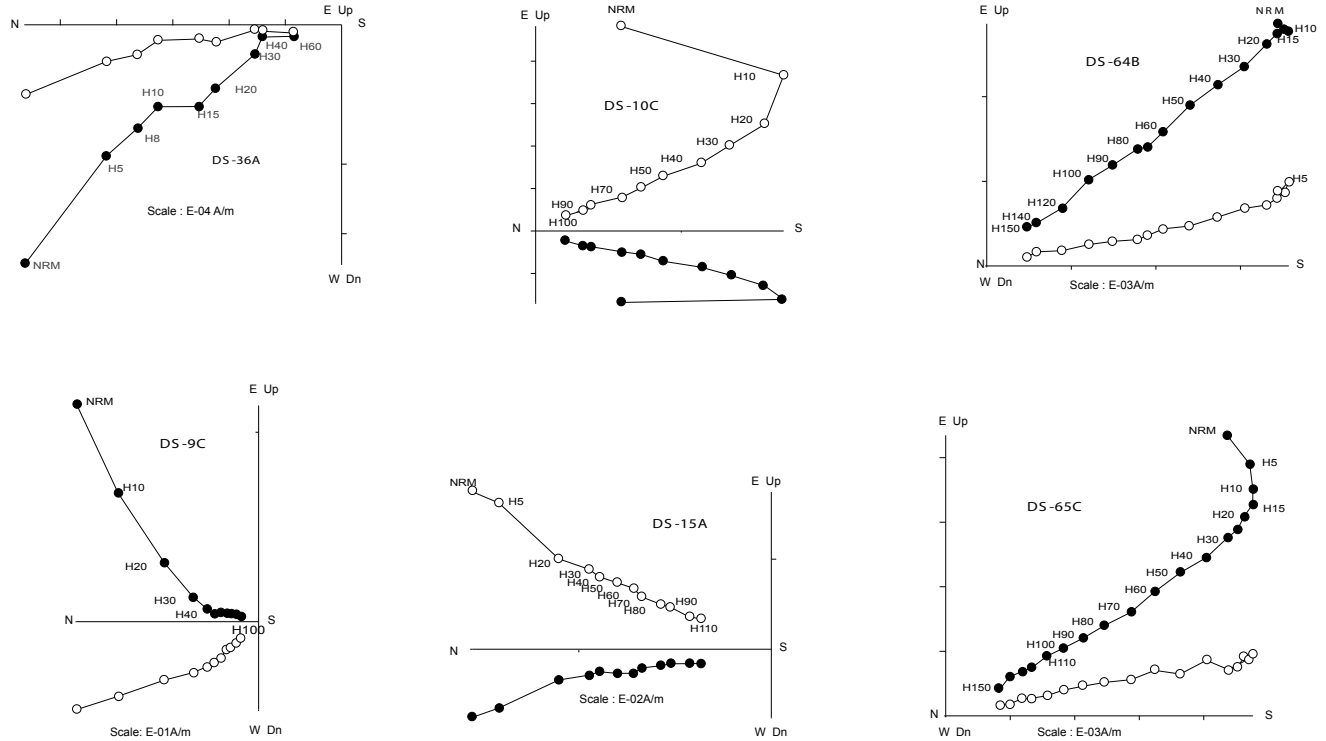

Figure 3: Orthogonal vector plots of AF demagnetization of representative samples. Solid circles indicate horizontal component; open circles indicate vertical component. Demagnetization steps in mT. NRM is the natural remanent magnetization.

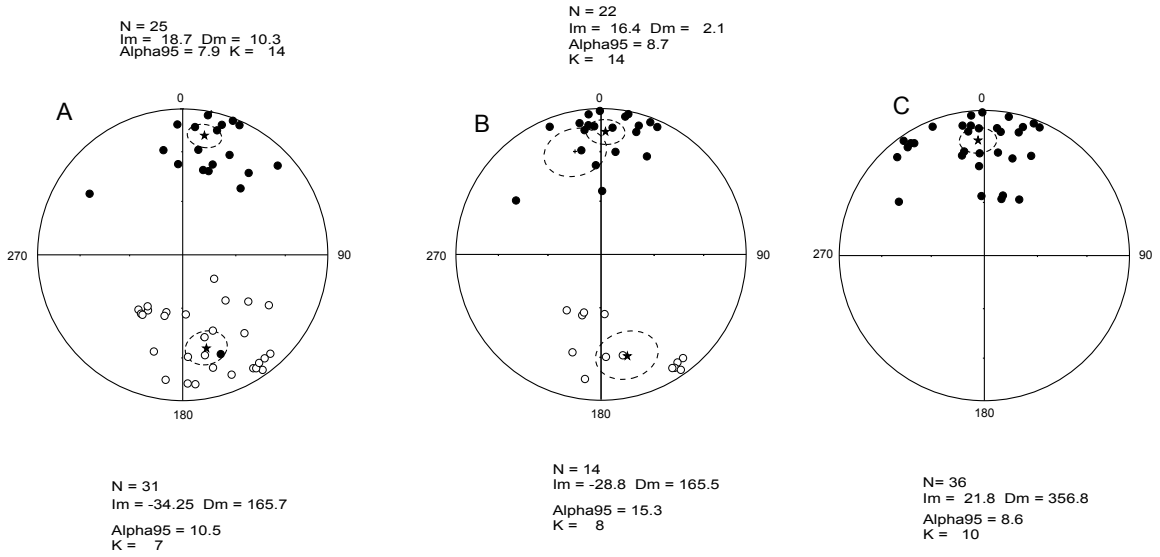

Figure 4: Equal-area stereographic projection of characteristic directions (normal and reversed polarities) isolated from samples. Circle around mean direction represents 95% confidence limit. A: mean direction for all normal and reversed samples. B: mean direction of normal and reverse drilled samples appear to be antipodal, and the reversal test is positive. C: mean direction of all drilled site (normal and reversed polarity) are plotted on the same hemisphere.

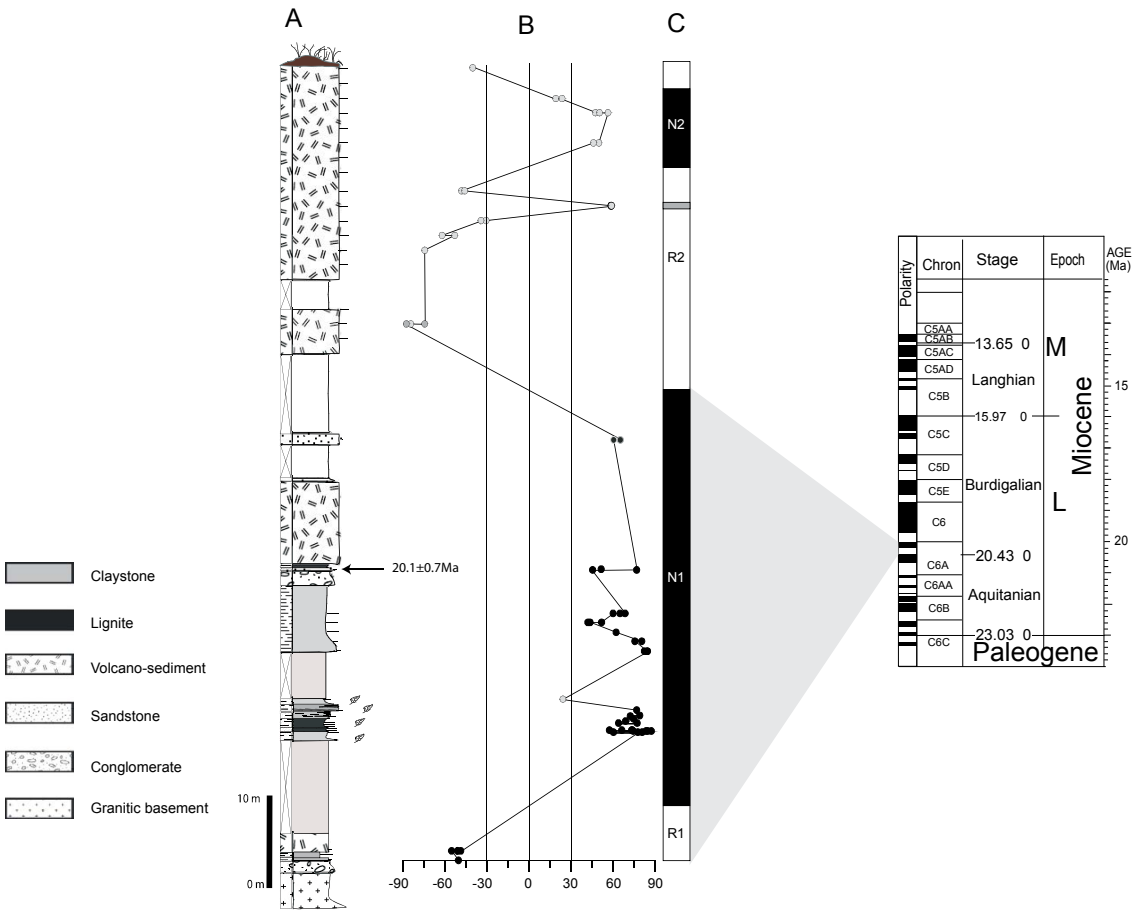

Figure 5: Lithology, magnetostratigraphy, and proposed correlation with the geomagnetic polarity time-scale. A: section and stratigraphic position of sampling sites. B: Positive and negative virtual geomagnetic pole (VGP) latitudes represent normal and reverse polarities respectively, gray dots correspond to hand bloc samples (C). D: Portion of the GPTS [27]. C: Polarity column (black/white bars represent normal/reverse polarity).

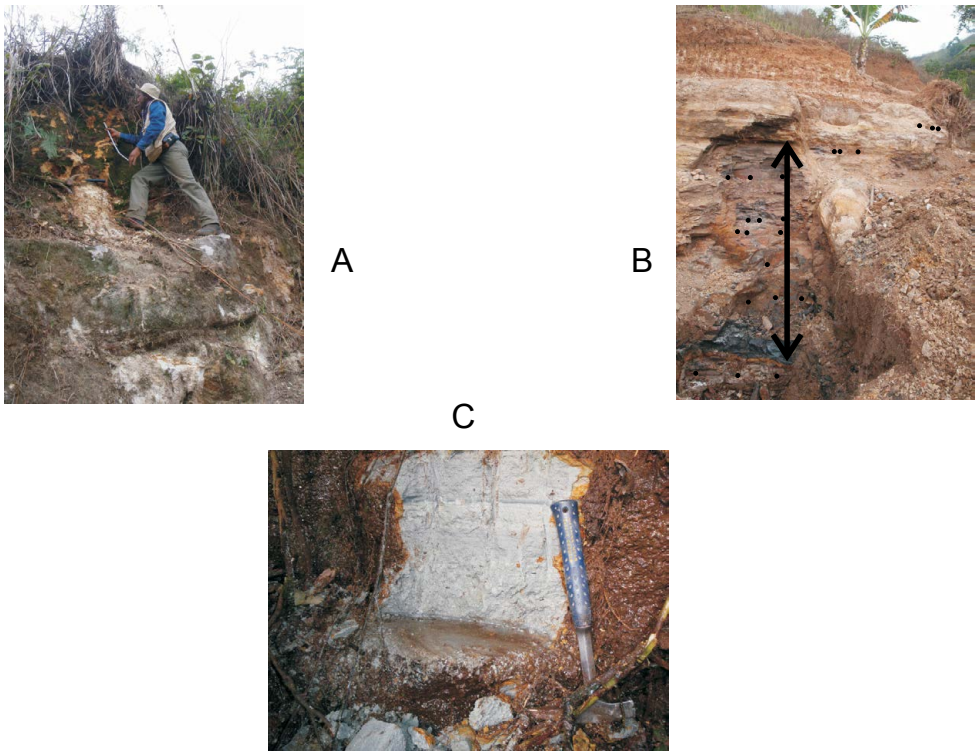

Figure 6: A) View of the lower part of the section with sandstone, conglomerate and grained yellowish tuff. B) View of the lignite layer, black dots indicates the paleomagnetic sampling. C) Volcanic tuff used for K-Ar dating.

a magnetic compass. Most drilled sites correspond to the lower part of the section. One or two orientated hand samples (blocks) were collected from the other 17 sites after digging to remove a lateritic soil that covers the formation. At each stratigraphic horizon described herein, a flat face was shaved on the in situ samples with a hand rasp, and then the strike and the dip of the face were measured with a Topochaix compass. Of the 17 originally sampled sites, 7 were lost during cutting or transport. The sampled lithology includes sandstones, tuff, clays and shale. One fresh sample about 15 m above the lignite seams was retained for radiometric determinations (Figure 6C).

Samples were analyzed in the paleomagnetic laboratory at the iPHEP (Institut de Paléoprimatologie, Paléontologie Humaine: Evolution et Paléoenvironnements) at the University of Poitiers. Remanent magnetization was measured with a JR6 magnetometer combined with stepwise thermal or alternating field demagnetization in a magnetically shielded room. To better constrain the magnetic mineralogy, we studied the acquisition of isothermal remanent magnetization (IRM), and then the stepwise thermal demagnetization of three-axis differential IRM following the method of Lowrie [20]. The specimens were subjected to stepwise thermal demagnetization in steps up to 600°C. The IRM was determined with a pulse electromagnet. Thermal demagnetization was done with a magnetic measurement thermal demagnetizer (*MMTD80*) shielded furnace. Progressive thermal demagnetization was carried out, in steps of 30°C to 40°C, from 100°C, until either the magnetization intensity fell below the noise level or the direction became erratic. The majority of specimens were submitted to stepwise alternating field (AF) demagnetization in increments of 5-10 mT, up to a maximum field of 150 mT using a Molspin Ltd. high-field shielded demagnetizer. Characteristic magnetization components were isolated by applying the method of Kirschvink [21] to vector segments composed of at least more than seven points with a maximum angular deviation of less than 15. Data resulting from AF demagnetization were plotted on orthogonal vector plots [22]. To determine characteristic magnetic directions, principal components analysis was carried out on all samples. These paleomagnetic directions were then analyzed, using Fisher statistics, to determine site mean declinations, mean inclinations, and associated precision parameters.

Radiometric dating

K-Ar analysis on tuff sample was conducted at the Instituto de Geología, UNAM (Univesidad Nacional Autonoma de Mexico). Plagioclase was obtained by crushing, sieving, selection of the best fraction (300-400 μm), washing, and separation by magnetic methods (Isodynamic Frantz separator). The K content was measured by XRF on 50 mg aliquots using a specific regression for measuring K in K-Ar samples [23]. Analytical precision was better than 2%. Duplicate samples weighing between 6 and 8 mg were degassed under high vacuum at ~150°C for twelve hours before analysis in order to reduce atmospheric contamination. Argon was extracted by complete sample fusion using a 50W CO_2 laser defocused to 1-3 mm of diameter. The evolved gasses were mixed with a known amount of 38Ar spike and purified with a cold finger immersed in liquid nitrogen and two SAES getters in a stainless steel extraction line. Measurements were done in static mode with an MM1200B mass spectrometer using electromagnetic peak switching controlled by a Hall probe. Analytical precision on ^{40}Ar and ^{38}Ar peak heights was better than 0.2%, and better than 0.5% on ^{36}Ar. The data was calibrated with internal standards and the international reference materials LP-6 and HD-B1 biotites. All ages were calculated using the constants recommended by Steiger and Jäger. A detailed description of the procedure and calculations can be seen in Solé [24].

Results

Magnetic properties and characteristic directions

A set of rock magnetic experiments was conducted to characterize and identify the magnetic mineralogy of the main lithologies. We first analyzed the acquisition of IRM (Isothermal Remanent Magnetization) up to 800 mT and its subsequent thermal demagnetization. Following the procedure described by Lowrie [20], magnetic fields of 1, 0.4 and 0.12 T were successively applied to each of the three perpendicular directions prior to thermal demagnetization. The IRM acquisition curves (Figure 2A) show a broad range of coercivities. The initial increase of magnetization up to 100-150 mT indicates the presence of low coercivity minerals. Saturation was not achieved at 800 mT, which indicates the presence of high coercivity minerals.

Thermal demagnetization shows that the low field (0.12 T) component is dominant and decreases up to a maximum unblocking temperature of approximately 580°C indicating magnetite as magnetic mineral (Figure 2B). The high coercivity component is present, and is unblocked at a maximum temperature of 350°C. This unblocking temperature is consistent with maghemite or Fe-sulfides as carrier. In Figure 3C and 3D, the first drop appears on the soft and medium components between 300°C and 350°C, indicating the existence of magnetic mineral with soft coercivity, probably corresponding to low-Ti titanomagnetite. The second drop is observed at 580°C indicating the presence of magnetite (Figures 2C and 2D). The harder components, less than 40% of the total IRM (Figure 2C), decrease regularly up to temperature of 300-350°C and suggest the presence of a Fe-sulphide (pyrrhotite or greigite).

The natural remanent magnetization displays moderately high values starting at 76×10^{-6} A/m in sandstone levels, and reaching up to ~ 6×10^{-3} A/m in the volcanic tuff; the majority of samples fall within the 1 to 10×10^{-3} A/m interval. The visual inspection of orthogonal demagnetization diagrams (Figure 3) reveals that the total NRM is generally composed of one or two components. For almost all of the samples, the individual characteristic remanent magnetization (ChRM) was clearly isolated. Nearly all samples are contaminated by a small secondary component, which is removed entirely completely between 10 and 40 mT and is therefore of recent origin. Characteristic remanent magnetization is generally removed at AF demagnetization between 10-40 mT and 100-150 mT (Figure 3). Demagnetization vector plots are generally of good quality, and in most cases, characteristic directions can be reliably determined.

The stable component, referred to as the characteristic remanent magnetization component (ChRM), shows both polarities: northerly declination with positive inclination and southerly declination with negative inclination (Figure 4). The mean direction was calculated separately for the normal polarity (Dec=10.3°; Inc=18.7°; k=14; K95=7.9) and for the reverse polarity (Dec=165.7°; Inc=-34.3; k=7; K95=10.5) (Figure 4A). The angular distance between the mean normal and reverse directions is 25.1° ± 9.6 and the 95% confidence circles about them do not overlap. Applying McFadden and McElhinny's reversal test (1990), this angle is greater than the critical angle at the 95% confidence level, so the reversal test is negative. The tow directions are not antipodal probably due to the strong overprint of the present day field which may not have been removed completely or due to the directions obtained from the blocs (may-be the blocs have been moved before sampling). The bedding attitudes of the formation do not allow the fold test to be applied because of the horizontal bedding of the strata. To limit the biasing effect we removed the bloc samples from the data set, the mean direction calculated for the normal polarity is (Dec=2.1°; Inc=16.4°; k= 14; K95=8.7) and for the reverse polarity is (Dec=165.5°; Inc=-28.8; k=8; K95=15.3) (Figure 4B). The α95 confidence cones overlap when plotted on the same hemisphere, and yield a class C positive reversals test [25] and indicates primary of the characteristic remanence. When all the sites mean directions (normal and reversed polarity) are plotted on the same hemisphere (Figure 4C), the mean declination is 356.8°, which indicates that since the time of deposition the Ngwa Formation has rotated 8° counter-clockwise. This rotation is probably related to the reactivation of the shearzone in the central part of the CVL which the Ngwa formation belongs to.

Magnetostratigraphic correlation and discussion

The ChRM directions of each sample were converted into virtual geomagnetic pole (VGP) latitude [26] with respect to the combined mean direction pole at 5.43 N, 10.08 E site coordinates. Based on VGP latitude, each level was assigned a polarity (Figure 5), and the data yielded the following results. The lower three sites representing 4 m thick have reverse polarity R1. Above these, and after a gap of about 10 m, the section continues with 30 m of normal polarity, followed by 26 m of reversed polarity. The last normal polarity N2 is represented by two sites that are 4 m thick. The question remains as to which part of the reversal time scale this series of reversals belongs to. The only independent mean of correlation available at the present time is the radiometric age. The K-Ar dates obtained from mineral concentrates yield an age of 20.1 ± 0.7 Ma on the tuff layer situated some 15 m above the lignite seam (Table 1). If we consider that remanent magnetization of the section we sampled is primary, we can compare our data with the geomagnetic polarity timescale GPTS. The chron C6An.1n in the lower part of the Burdigalian stage lasts 0.17 my; it lies between 20.04 and 20.21 Ma [27], which means that our normal polarity N1 can be correlated with chron C6An.1n, and the reversed polarity R1 can be correlated with chron C6An.1r. If we exclude the data obtained from the hand bloc samples, the proposed correlation does not change.

Conclusion

This study has provided paleomagnetic and rock magnetic results of the Ngwa Formations and indicates that the dominant detrital magnetic minerals are titanomagnetite, magnetite and Fe-sufides. The characteristic magnetization is primary based on the positive reversal test, mean polarity direction counter-clockwise in respect with expected directions for the Lower Miocene of Africa. Magnetostratigraphic analysis and K-Ar age demonstrate that the lignite of Ngwa Formation can be correlated with chron C6An.1n and has an age comprised between 20.0 and 20.2 Ma. Using the magnetostratigraphic data and age estimates for the duration of the magnetic polarity chrons, we have, for the first time determined the age of the lacustrine lignite of Ngwa Formation.

Acknowledgements

We sincerely thank the IRGM Authority for providing logistic and technical assistance with field work, as well as Mathieu Schuster, Guy Franck, and Xavier Valentin. The research reported in this paper was supported by ANR-09-BLAN-0238-02 program. We are very grateful to Teodoro Hernández Treviño for assistance in mineral separation

References

1. Petters SW, Okereke CS, Nwajide CS (1987) In: Matheis G, Schandelmerer H (Eds.) Geology of the Mamfe rift, southeastern Nigeria. Current research in African earth sciences, Balkema, Rotterdam p299-302.
2. Nguimbous-Kouoh JJ, Takam Takougang EM, Nouayou R, Tabod C, Manguelle-

Dicoum E (2012) Structural Interpretation of the Mamfe Sedimentary Basin of Southwestern Cameroon along the Manyu River Using Audiomagnetotellurics Survey. ISRN Geophys 413042: p. 7.

3. Njike PR, Eno BSM, Ndjeng E, Hell JV, Tsafack JPF (2000) Contexte tectonogénique de la mise en place des basins sédimentaires camerounais du Sud au Nord. J Geosci Soc Cameroon GSAf12: Geo-environmental catastrophes in Africa. Abstract pp: 96-97.
4. Touatcha MS, Richard NNP, Salah MM, Said DA, Emmanuel EG (2010) Existence of "late continental" deposits in the Mbere and Djerem sedimentary basins (North Cameroon): Palynologic and stratigraphic evidence. J Geol Min Res 2: 159-169.
5. Dejax J, Michard JG, Brunet M, Hell J (1989) Empreintes de pas de dinosauriens dates du Crétacé inférieur dans le bassin de Babouri-Figuil (Fossé de la Bénoué, Cameroun). N Jb Géol Paläont Abh 178: 85-108.
6. Brunet M, Dejax J, Brillanceau A, Congleton J, Downs W, et al. (1988) Mise en évidence d'une sédimentation précoce d'âge Barrémien dans le fossé de la Bénoué en Afrique occidentale (Bassin du Mayo Oulo Léré, Cameroun), en relation avec l'ouverture de l'Atlantique Sud. CR Acad Sci Paris Série 306: 1125-1130.
7. Ndjeng E, Brunet M (1998) Modèles d'évolution géodynamique de deux bassins de l'Hauterivien-Barrémien du Nord-Cameroun: Les bassins de Babouri-Figuil et du Mayo Oulo-Léré (Fossé de la Bénoué). Géoscience au Cameroun, Presse Univ. Yaoundé I pp: 163-165.
8. Stendal H, Toteu SF, Frei R, Penaye J, Njel UO, et al. (2006) Derivation of detrital rutile in the Yaounde region from the Neoproterozoic Pan-African belt in southern Cameroon (Central Africa). J African Ear Sci 44: 443-458.
9. Dejax J, Brunet M (1996) Les flores fossiles du bassin d'Hama-koussou, Crétacé inférieur du Nord-Cameroun: corrélations biostratigraphiques avec le fossé de la Bénoué, implications paléogéographiques. Géologie de l'Afrique et de l'Atlantique Sud. Actes Colloques Angers. Bulletin Centres Recherches Exploration-Production Elf-Aquitaine 16: 145-173.
10. Bessong M, El Albani A, Hell JV, Fontaine C, Ndjeng E, et al. (2011) Diagenesis in Cretaceous Formations of Benue Trough in the Northern Part of Cameroon: Garoua Sandstones. World J Eng Pure Appl Sci 1: 58-67.
11. Kenfack PL, Tematio P, Kwekam M, Gabriel N, Njike PR (2011) Evidence of a Miocene volcano-sedimentary lithostratigraphic sequence at Ngwa (Dschang Region, West Cameroon): Preliminary analyses and geodynamic interpretation. J Petrol Tech Alter Fuels 2: 25-34.
12. Capponi A (1945) Le lignite de Dschang. Bull Soc Et Camerounaises 7: 75-86.
13. Marzoli A, Piccirillo EM, Renne PR, Bellieni G, Iacumin M, et al. (2000) The Cameroon volcanic line revisited: Petrogenesis of continental basaltic magma from lithospheric and asthenospheric mantle sources. Oxford University Press pp: 87-109.
14. Déruelle B, Moreau C, Nkoumbou C, Kambou R, Lissom J, et al. (1991) In: Kampunzu AB, Lubala RT (Eds.) The Cameroon Line: a review. Magmatism in Extensional Structural Settings: The Phanerozoic African Plate. Springer-Verlag, Berlin pp: 274-327.
15. Nono A, Njonfang E, Kagou Dongmo A, Nkouathio DG, Tchoua FM (2004) Pyroclastic deposits of the Bambouto volcano (Cameroon Line, Central Africa): evidence of an initial strombolian phase. J African Ear Sci 39: 409-414.
16. Dongmo AK, Wandji P, Pouclet A, Vicat JP, Cheilletz A, et al. (2001) Evolution volcanologique du mount Manengouba (ligne du Cameroun), nouvelles données pétrographiques. CR Acad Sci Paris Série 333: 155-162.
17. Dongmo AK, Nkouathio D, Pouclet A, Bardintzeff JM, Wandji P, et al. (2010) The discovery of late Quaternary basalt on Mount Bambouto: Implications for recent widespread volcanic activity in the southern Cameroon Line. J African Ear Sci 57: 96-108.
18. Youmen D, Schmincke HU, Lissom J, Etame J (2005) Données géochronologiques: Mise en évidence des différentes phases volcaniques au Miocène dans les Monts Bambouto (Ligne du Cameroun). Sci Technol Dev 11: 49-57.
19. Nkouathio DG, Dongmo AK, Bandintzeff JM, Wandji P, Bellon H, et al. (2008) Evolution of volcanism in graben and horst structure along the Cenozoic Cameroon Line (Africa): implications for tectonic evolution and mantle source composition. Mineral Petrol 94: 287-303.
20. Lowrie W (1990) Identification of ferromagnetic minerals in a rock by coercivity and unblocking temperature properties. Geophys Res Lett 17: 159-162.
21. Kirschvink JL (1980) Least-squares lines and plane the analysis of paleomagnetic data. Geophys J Int 62: 699-718.
22. Zijderveld JDA (1967) In: Collinson DW, Creer KM, Runcorn SK (Eds.) AC demagnetization of rocks: Analysis of results, Methods in Paleomagnetism: Amsterdam, Netherlands, Elsevier pp: 254-286.
23. Solé J, Enrique P (2001) X-ray fluorescence analysis for the determination of potassium in small quantities of silicate minerals for K-Ar dating. Analytica Chimica Acta 440: 199-205.
24. Solé J (2009) Determination of K-Ar ages in milligram samples using an infrared laser for argon extraction. Rapid Commun Mass Spectrom 23: 3579-3590.
25. McFadden PL, McElhinny MW (1990) Classification of the reversal test in palaeomagnetism: Geophys J Int 103: 725-729.
26. Opdyke ND, Channell JET (1996) Magnetic Stratigraphy, Academic Press, San Diego, California, USA p. 345.
27. Gradstein FM, Ogg JG, Smith AG (2004) A Geologic Time Scale 2004, Cambridge, UK, Cambridge University Press. p. 589.